Time Dependence of Settlements

Jacobsen, Moust

Published in:
Bulletin No. 27

Publication date:
1970

Document Version
Publisher's PDF, also known as Version of record

Time Dependence of Settlements

Consolidation settlements of buildings founded on clay or clayey soils are assumed to consist of two simultaneous phases. The first one is the so-called primary consolidation, due to drainage. The second phase is the so-called secondary consolidation, which is a creeping effect. Only loadings smaller than 25 % of the ultimate bearing capacity will be treated here. In paper 2 is mentioned, that this corresponds to normal engineering practice, when dealing with moraine clay.

The construction period for a building founded on a moraine clay is normally much longer than the consolidation period, because the permeability of a moraine clay is rather great compared with that of a normal clay. In order to investigate this some plate tests have been carried out with controlled loadings applied in discrete increments, and time curves have been observed. The first part of these time curves, where the primary consolidation dominates, is nearly proportional to the square root of time and the second part, where the creep effect makes itself most strongly felt, is normally proportional to the logarithm of time. The time curve is therefore most appropriately plotted in a composite $\sqrt{t}$, log t diagram as proposed by Brinch Hansen (1961). A time curve is shown in fig. 3.1.

This chapter deals mainly with the problem of calculating the consolidation time t_c, as defined in fig. 3.1.

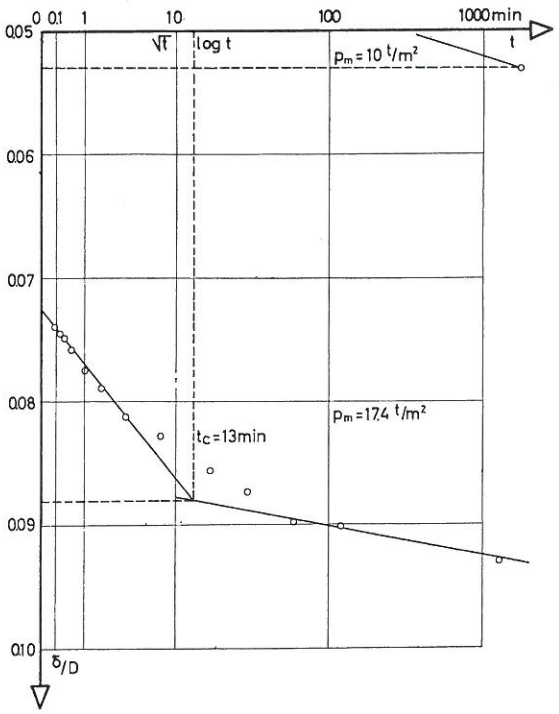

Fig. 3.1 A typical time curve for plate test.
The diameter of the plate is 0.5 m. Kratbjerg moraine clay.

Introduction

The coefficient k is determined in an ordinary oedometer. Terzaghi's well-known solution gives

$$k = \frac{\pi}{4} \cdot \frac{\gamma_w H^2}{K t_c} \tag{3.1}$$

where K is a modulus of compressibility ($K = 1/m_v$), t_c is the consolidation time as previously defined, and H is the drainage path. In oedometers with parallel pore water flow to both ends of the specimen H is half the sample height; in the new oedometer described in Paper 1 an equivalent drainage path $H_q = 0.7\ D$ has to be used.

In plate tests and under circular footings the drainage is axi-symmetrical. Using the theory of elasticity an equivalent drainage path H_q can be estimated by means of EDP-analyses.

In the following, three groups of assumptions and questions involved in the problem are treated:

1 Determination of the coefficient of permeability k assumes that:

1.1 The oedometer allows measurement of deformations and time rates.

1.2 The water flow through the clay obeys Darcy's law of permeability: $v = k \cdot i$. k is the coefficient of permeability and is a constant, independent of stress level and the amount of pore water flow.

1.3 The modulus of compressibility K is a constant, independent of the stress level.

1.4 The clay is fully saturated. This means that the liquid phase is incompressible compared with the clay skeleton under drained conditions, and that the excess pore water pressure u is equal to the difference between the total applied load and the effective pressure: $u = \sigma - \bar{\sigma}$.

2 Calculations of t_c for foundations on the basis of the theory of elasticity poses the problems:

2.1 Boundary conditions for drainage:
Permeable or impermeable base.

2.2 Boundary conditions for deformations.
Rigid or flexible foundation.

3 Deviations from the theory of elasticity may be:

3.1 The stiffness of the soil depends on the overburden pressure.

3.2 Expansion before rupture.

Permeability of Saturated Samples

The influence of the apparatus

If the consolidation time t_c is shorter than one minute, it is very difficult to estimate the time rate be-

cause the first observations are relatively more doubtful than those taken later. In the new oedometer the drainage path $H_q = 5$ cm is big enough to obtain time curves of a reasonable length as can be seen in fig. 3.2. Here t_c is 18 min.

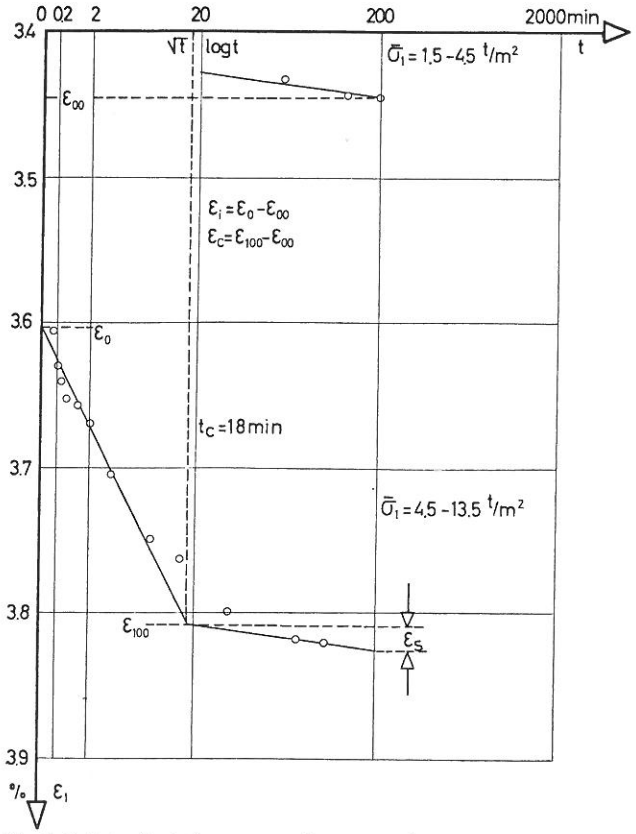

Fig. 3.2 A typical time curve for an oedometer test. Kratbjerg moraine clay.

The permeability of Kratbjerg moraine clay determined in the new oedometer is

$$k = 5.1 \cdot 10^{-10} \text{ m/sec (60 observations)}$$

In an oedometer with a drainage path of 1 cm only the result of 25 rebound and recompression time curves is

$$k = 0.6 \cdot 10^{-10} \text{ m/sec}$$

but here an initial compression caused by air in the sample is overestimated.

Darcy's law

The validity of Darcy's law can be investigated in permeability tests. The measurement of pore water flow at different gradients gives further information on the nature of the flow, and the influence of the amount of water flowing through the specimen can also be examined.

The micro structure of the soil has a great effect on the results, and some differences between normal clays and moraine clays should therefore first be pointed out.

A normal fat clay consists of clay flakes with water filling the spaces between the flakes. A water molecule is an electric dipole. These dipoles can be bound to each other and to ions at the mineral surface in a nearly rigid lattice in an undisturbed clay. This binding of pore water molecules is most active near the clay mineral surface and it becomes weaker when the distance to the mineral surfaces increases. Normally most of the pore water is more or less bound. In flowing water the dipoles are not orientated and the water gives an irregular alternating current, which disengages the most loosely bound water. The permeability might thus be expected to increase with an increasing amount of pore water flow. The pore water flow might also be expected to be relatively small at a small gradient, which means that for bigger gradients Darcy's law may be modified to

$$v = k\,(i - i_o)$$

where i_o is the so-called threshold gradient. For smaller gradients $i/i_o < 3$ to 5 this expression can be replaced by an exponential function as proposed by Hansbo (1960).

Florin (1959) has analysed some permeability tests performed by Rosa and he found that the threshold gradient is as high as 17–30. He found further that vibrations influenced the results very much and in some tests i_o fell to zero.

Hansbo (1960) has made very carefully performed tests in a special apparatus. He found that i_o is less than 2, in one case $i_o = 0$. He used only very small amounts of water during a test; normally only 1 % of the pore water was exchanged.

Moraine clay is a system of sand grains, clay flakes and pore water. The clay flakes are situated in corners between the sand grains, preventing the water from flowing there. The water therefore probably flows mostly between the sand grains, which are unelectric, and the phenomena described above are connected only with the clay phase. It may therefore be supposed that the results of permeability tests carried out on a normal clay and the results of those on moraine clay are not directly comparable.

Permeability tests

A permeability test is performed in a special apparatus. A pressure difference between two filter discs covering the top and the bottom surfaces of a sample causes a flow of water through the sample. The pressure difference is kept constant during the consolidation of the sample and afterwards during the measurement of pore water flow. In each test several levels of pressure difference are used. The water in the system is de-aired in order to avoid air-bubbles in the filters. Before measurement takes place the filter system is very carefully de-aired.

Permeability tests at very small stress levels are strongly influenced by a consolidation of the sample, caused by changes in the gradient and taking very long time. For decreasing gradients tests show, that the pore water flow does not follow Darcy's law and that the so-called threshold gradient i_o is as high as 20–30. But for increasing gradients i_o seems to be very small.

To avoid this source of error the permeability is investigated at higher stress levels. The sample is placed between two filter discs and covered with a thick membrane, reinforced by steels rings. The membrane is greased inside to prevent the water from flowing along it. There is no movement between ring and pressure heads and it is thus possible to make the apparatus impervious.

Measurement of water flow takes place in horizontally mounted capillary tubes by means of air-bubbles at least 10 mm in length. In the first version of the apparatus the flow into the sample as well as the flow out of the sample was measured.

The apparatus was first calibrated without a sample and the filter discs pressed against each other. The

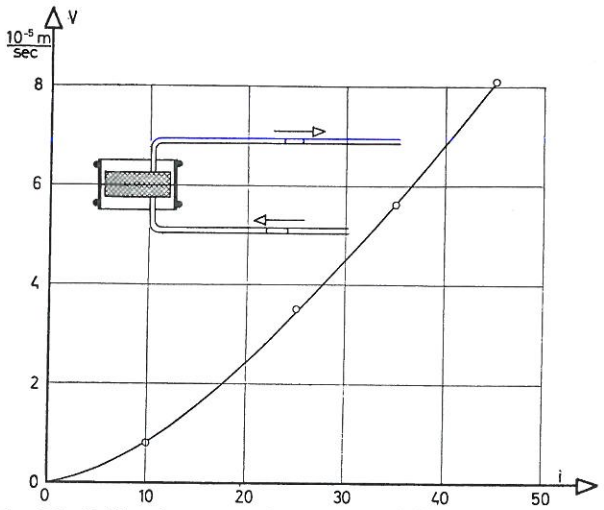

Fig. 3.3 Calibration curve for a permeability test apparatus. The gradient is calculated according to a fictive sample, height of 2 cm.

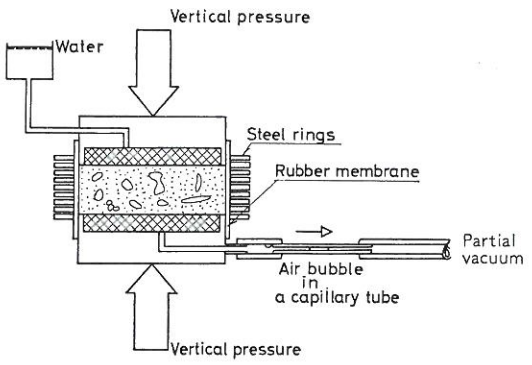

Fig. 3.4 The apparatus used for permeability measurements shown in figs. 3.5 and 3.7.

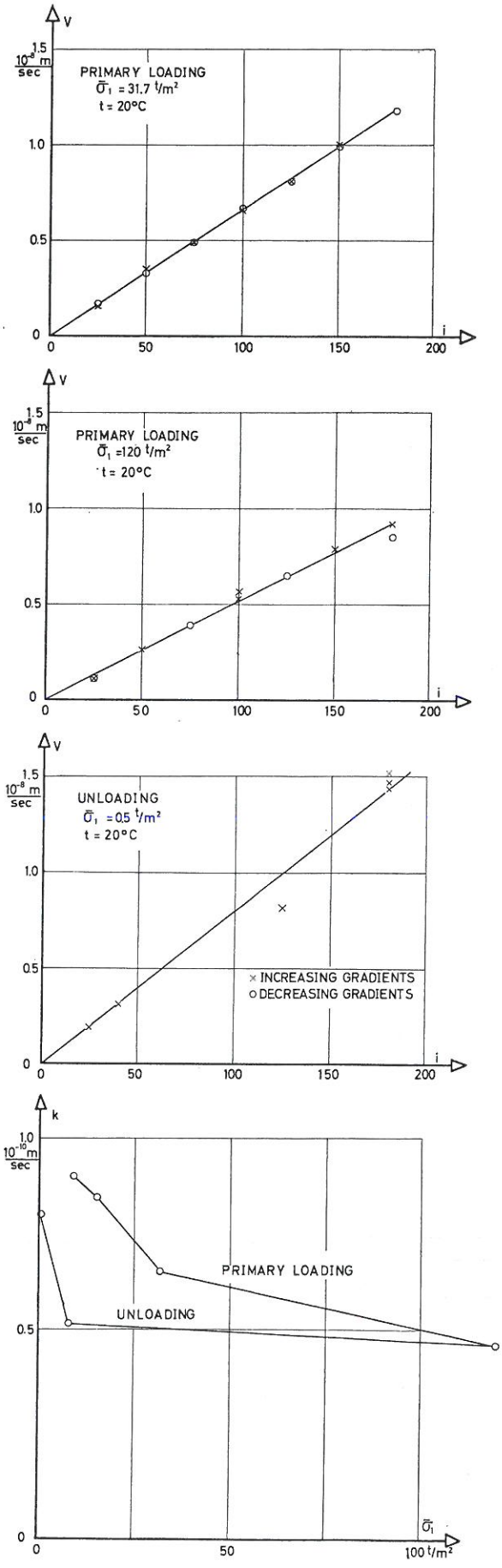

Fig. 3.5 Permeability tests on Kratbjerg moraine clay.

pressure difference was changed several times. The hydraulic gradient i was calculated according to a fictive sample height of 20 mm. The results are shown in fig. 3.3. They indicate that the apparatus itself has a threshold gradient. When we measured the water flow through a sample obeying Darcy's law of permeability it appeared that threshold values increased, when the permeability grew. The conclusion was that the tubes had to be as short and thick as possible. This was tested in a new series. Consequently a new bubble had to be produced before each measurement.

A sketch of the apparatus is shown in fig. 3.4. Using a preconsolidated sample a vacuum can be applied to the system after mounting the sample in order to evacuate air from the filter system. The vacuum is applied several times but lasts only for a few minutes to prevent change in the degree of saturation.

During the test, suction in the flowing pore water gives the pressure difference. Thus a leakage gives air bubbles in the measuring system. For each gradient measurements are made so many times that variations in the results are fortuitous.

Some of the test results can be seen in fig. 3.5. The test was carried out on Kratbjerg moraine clay. The cross-section area of the sample was 38.5 cm². It will be seen that the threshold gradient is very small and that the results agree with Darcy's law. The coefficient of permeability varies only by a factor of two.

Prolonged tests

Hansbo only used very small amounts of water during a test. By turning the flow direction he managed to have only 1 % of the pore water replaced by new water.

Some tests were carried out on nearly saturated moraine clay specimens with the purpose of finding the dependence between permeability and the amount of water flow. First a normal test as described above was performed, followed by a prolonged pore water flow, and afterwards again new measurements were made. Fig. 3.6 shows that the amount of pore water flow has only a small effect on the permeability of moraine clay.

A prolonged test on a fat clay showed, however, a great effect on the coefficient of permeability.

Oedometer tests

During each loading step k and K vary somewhat. In order to investigate the influence of these variations on the determination of k some tests have been carried out on nearly saturated samples. First some permeability tests also including Little Belt clay were performed, and after that oedometer tests with parallel drainage on the same specimens. The results can be compared directly as may be seen in fig. 3.7. This shows that the determination of k is scarcely influenced by varying K and k.

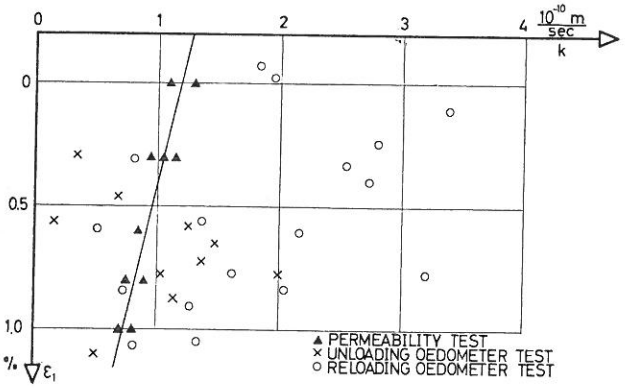

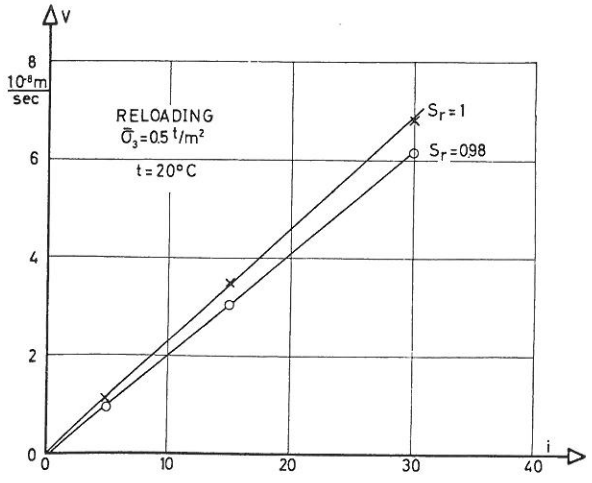

Fig. 3.6 Permeability test on Kratbjerg clay. Full saturation is managed by prolonged water flow.

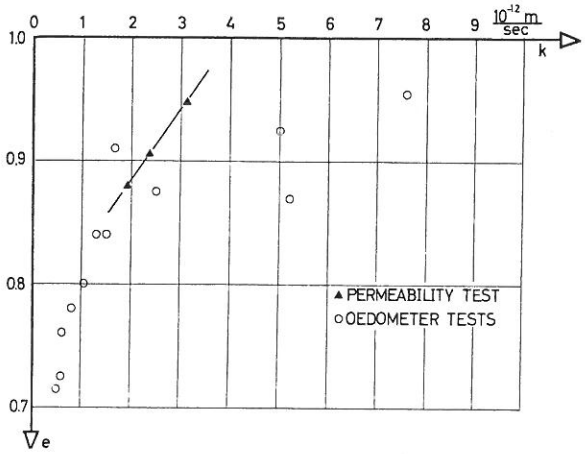

Fig. 3.7 Permeability test and oedometer tests performed on the same specimen. Kratbjerg moraine clay and Little Belt clay.

Permeability of Unsaturated Samples

As mentioned earlier, moraine clay samples are normally unsaturated after sampling and preparation, although moraine clay is normally saturated in the natural state. This means that air bubbles situated between the grains make the water flow difficult. Thus the permeability measured in the laboratory may be too low.

Permeability Tests

In order to investigate this effect some tests were performed in a triaxial cell. A sample was placed between filter discs with a short membrane covering its surface. A longer membrane outside the short one also covered the filter discs and end platens. If the pressure in the measuring system is greater than that in the cell the long membrane will grow bigger and permit the water to flow around the sample between the membranes (fig. 3.8). Just before the test this was done for half a minute and the air got out of the filters without affecting the degree of saturation of the sample. The void ratio and degree of saturation were determined by the bulk density method. (Described in Paper 1).

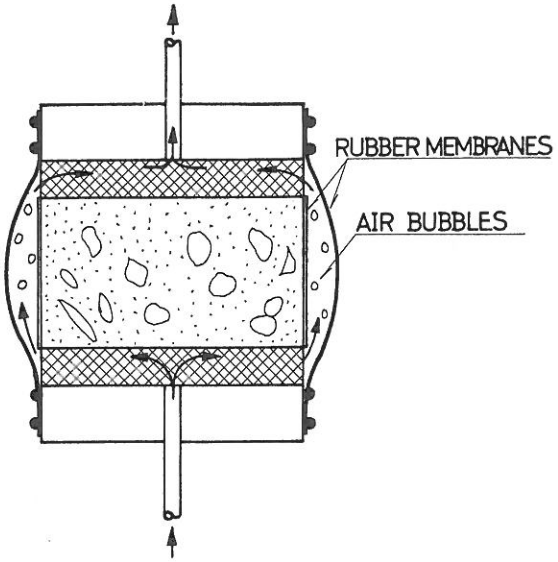

Fig. 3.8 Permeability test apparatus used in a triaxial apparatus when performing tests on unsaturated samples. Tests in this apparatus are shown in figs. 3.6, 3.9 and 3.10.

After measurement of the coefficient of permeability the water flows through the sample for one or two days. In this way the air is exhausted from the sample. Afterwards a new series of measurements takes place.

Fig. 3.9 shows two tests. Assuming that the duration and amount of water flow have no influence, as verified earlier, it is possible to compare the permeability at the actual degree of saturation with that of a fully saturated sample.

The results can be seen in fig. 3.10, showing that if $S_r = 0.9$ in the laboratory the natural permeability is twice as great as that measured. Table 3.1 shows the results of permeability tests with saturated samples.

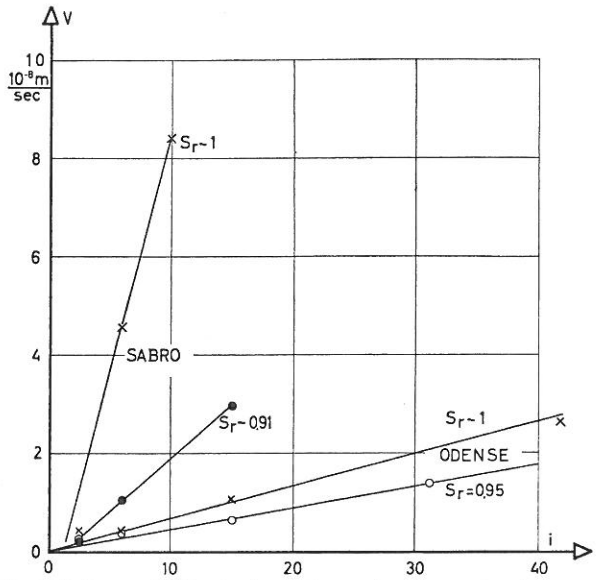

Fig. 3.9 Permeability tests performed on unsaturated samples. After the first test series the samples are saturated by means of prolonged water flow.

TABLE 3.1

Permeability tests. $S_r = 1$

Locality	$\bar{\sigma}$, t/m²	k, 10^{-10} m/sec
Sabro	0.5	28
	0.5	22
	0.5	80
	10	15
	20	18
	5	18
Kratbjerg	0.5	40
	0.5	23
	0.5	20
Odense	0.5	6.5

Oedometer Tests

When calculating the coefficient of permeability by means of oedometer tests as if the sample were fully saturated, we got a wrong result. But fig. 3.10 could not be used to correct the results even if the saturation degree was measured, because it describes a different phenomenon.

In a permeability test the air bubbles prevent the water from flowing, but in the oedometer test they cause elasticity in pore water. At the start of a time curve the air bubbles are compressed and cause an initial deformation, as can be seen by a time curve in

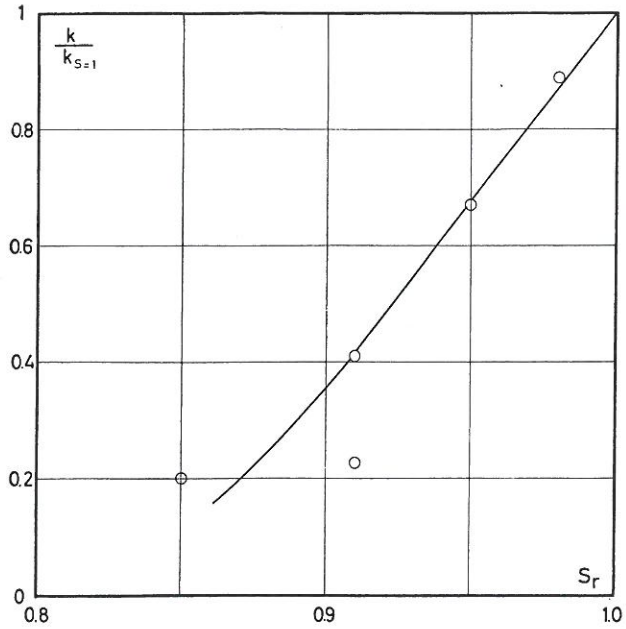

Fig. 3.10 The influence of the degree of saturation on the measurement of the coefficient of permeability in permeability tests.

fig. 3.2. Later on the air bubbles grow bigger again as the pore water pressure decreases, but it is not possible to measure this effect.

In order to calculate the real permeability of the sample nearly corresponding to the fully saturated state, we have to make simplifying assumptions, which shall be discussed later on:

1. Even in unsaturated clays the pore water pressure u is equal to the differences between total and effective stresses.
2. The liquid phase, i.e. water and air, is elastic:

$$\varepsilon_L = \frac{1}{L} \cdot \gamma_w \cdot h \tag{3.2}$$

where ε_L is the compression of the liquid phase, relative to the total volume of the system, h the hydraulic potential, and L a modulus of compressibility.

The system under consideration consists now of three phases:

1. The soil phase. The compression of this is given by

$$\sigma_1 = \bar{\sigma}_1 + u = K \cdot \varepsilon_1 + \gamma_w \cdot h \tag{3.3}$$

2. The water phase, being unelastic. The decrease of pore water volume is called ε_p.
3. The air and vapour phase. The compression of this can be found by (3.2).

Further we have:

$$\varepsilon_1 = \varepsilon_p + \varepsilon_L \tag{3.4}$$

During consolidation the total normal stresses are constant. (3.3) gives the differential equation:

$$K \cdot \frac{\delta \varepsilon_1}{\delta t} + \gamma_w \cdot \frac{\delta h}{\delta t} = 0 \tag{3.5}$$

The water flow is given by Darcy's law:

$$v = k \cdot i = -k \cdot \frac{\delta h}{\delta z}$$

Consider a parallel water flow through an elemental volume of clay of a height dz, the water being squeezed out from the voids during vertical loading with no lateral yield of the clay. The rate of decrease of pore water volume ε_p is equal to the rate of changing of flow through the end surfaces:

$$\frac{\delta \varepsilon_p}{\delta t} = \frac{\delta v}{\delta z} = -k \cdot \frac{\delta^2 h}{\delta z^2} \tag{3.6}$$

Just after the new load is applied ($t = 0$), an initial deformation ε_i is caused by compression of the air and vapour phase as expressed by (3.2). At the end of consolidation ($t = t_c$) this compression is relieved, the soil phase is now deformed by $\varepsilon_1 = \varepsilon_c$, and the value of σ_1 by (3.3) is unchanged. Using (3.2) and (3.3) first for $\varepsilon_1 = \varepsilon_L = \varepsilon_i$ and then for $\varepsilon_1 = \varepsilon_c$, $\varepsilon_L = 0$ we find:

$$L = \frac{\varepsilon_c - \varepsilon_i}{\varepsilon_i} K \tag{3.7}$$

This means that by determining the initial deformation, we can find L.

$\varepsilon_c - \varepsilon_i$ is the deformation caused by water flow. It can be seen that when testing a stiff soil the initial deformation makes up a great part of the total deformation ε_c. (K is very great for stiff soils).

The differential equation for the drainage can be found by (3.4), (3.5), and (3.6):

$$\frac{\delta h}{\delta t} = \frac{k \cdot K}{\gamma_w} \left(\frac{1}{1 + K/L} \right) \cdot \frac{\delta^2 h}{\delta z^2}$$

Now equation (3.7) can be used:

$$\frac{\delta h}{\delta t} = \frac{\varepsilon_c - \varepsilon_i}{\varepsilon_c} \cdot \frac{k \cdot K}{\gamma_w} \cdot \frac{\delta^2 h}{\delta z^2}$$

If we replace k with another constant $k_c = \frac{\varepsilon_c - \varepsilon_i}{\varepsilon_c} \cdot k$ we get the normal equation for drainage:

$$\frac{\delta h}{\delta t} = c_c \frac{\delta^2 h}{\delta z^2} \tag{3.8}$$

c_c is a corrected coefficient of consolidation.

This means that the solution of this problem is the same as given earlier (e.g. Taylor 1948) except for the time of consolidation being $\frac{\varepsilon_c}{\varepsilon_c - \varepsilon_i}$ times longer.

It will be seen that the real advantage of using this method is that the influence of the degree of saturation S_r is taken into account by determining the initial deformation ε_i. S_r normally increases during a test and it is thus not possible to measure it directly.

This method involves some new assumptions and can of course not be accepted without further comments.

Bishop showed in 1963 that for unsaturated clays a better assumption (instead of assumption 1) is

$$\bar{\sigma} = \sigma - [u_a - \chi(u_a - u_w)] \qquad (3.9)$$

where u_a denotes pressure in the air and vapour phase and u_w denotes pressure in the pore water. Bishop and Blight (1963) showed some measurements of χ, among several tests also a test on a moraine. This can be seen in fig. 3.11. All the samples under consideration have a degree of saturation $S_r > 0.85$, and in this case it seems to be a good approximation that $\chi = 1$, which means that $\bar{\sigma} = \sigma - u_w$.

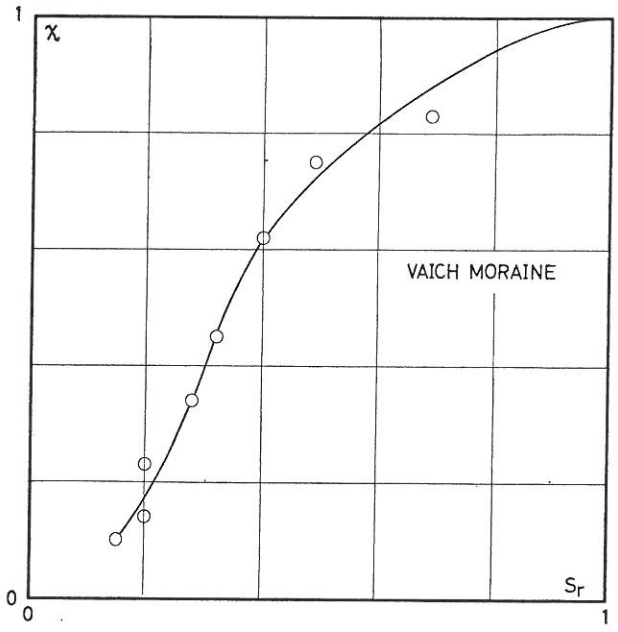

Fig. 3.11 Test results, published by Bishop and Blight in 1963. The curve is drawn by the author.

When loading a sample the excess pore water pressure increases and the air bubbles decrease, some of them being dissolved in the pore water. During the first part of consolidation most of the gas bubbles flow away with the pore water, if S_r is big enough. During the last part of the primary consolidation the gas bubbles again increase and separate from the water, some of them preventing flow of water. Using Brinch Hansen's $\sqrt{t}$, log t plot only the first and last parts of the consolidation curve are used, and therefore the prevention of water flow normally has no effect.

However, when unloading a sample the gas bubbles expand, and then the water flow is obstructed. The water flow takes too long and this calculation method cannot be used.

The compression of the air and vapour phase can approximately be calculated by means of Boyle-Mariotte's law combined with Henry's law, if tensions in the surfaces of the bubbles are disregarded. According to these laws $p \cdot V_L$ is constant, if the temperature is constant, and the amount of an idealized gas dissolved in a fluid at constant temperature is proportional to the gas pressure. Henry's constant is $H = 2\ \%$ (by volume) per at.

Combining these laws we get:

$$\varepsilon_a = \frac{p_1 - p_o}{p_1}\left(1 + p_o H \frac{S_r}{1 - S_r}\right)$$

where ε_a is the relative decrease of the volume of air, p_o the absolute atmospheric pressure and p_1 the actual pressure.

From the definitions of ε_a and ε_L it follows that

$$\varepsilon_a = \varepsilon_L \cdot \frac{e+1}{e}\frac{1}{1-S_r}$$

The air will be totally dissolved in the water, i.e. $\varepsilon_a = 1$, when $p_1 - p_o = \frac{1}{H}\frac{1-S_r}{S_r}$. Fig. 3.12 shows ε_a for three different degrees of saturation. In a usual test on moraine clays with load increments less than 60 t/m², only the thick lines are used. It may therefore be seen that assumption 2 is quite as good as the usual one: K and k are constants.

This method is therefore used under the following conditions:

1. $S_r > 0.85$ before the test.
2. Reloading curves with $\Delta\bar{\sigma} < 60$ t/m².

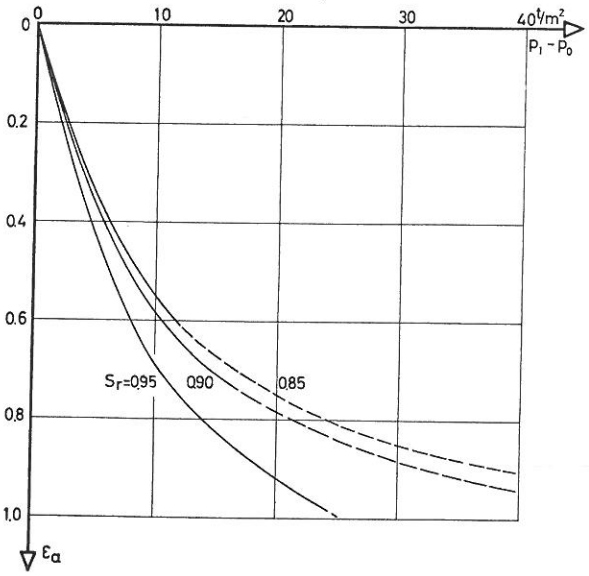

Fig. 3.12 The compression of the liquid phase calculated by means of Boyle-Mariotte's law and Henry's law.

In table 3.2 are seen the coefficients of permeability for different moraine clays as determined in the normal way (k) and with corrections according to the new method (k_c). The mean effect of this correction gives a factor of about 3.

The degree of saturation before the test cannot be determined because the volume is unknown, but the mean value of it after the test is 0.93. The degree of saturation during the test is probably somewhat smaller, so by comparing the present results with those of fig. 3.10 from permeability tests in a triaxial cell it can be seen that the influence of air bubbles in the pore water has been nearly the same as in the determination of the permeability by oedometer tests.

TABLE 3.2

Oedometer test results. Recompression curves

Locality	Lab. no.	Numbers of tests	k 10^{-10}m/sec	k_c 10^{-10}m/sec
Sabro	36	11	3.7	14.2
	37	13	3.4	10.9
	38	11	12.8	48
	39	8	17.9	76
	41	8	9.2	40
	43	7	5.6	25.8
Kratbjerg	3	6	2.2	6.8
	5	10	3.0	8.4
	6	7	3.3	15.1
	12	10	7.8	21.4
	13	9	7.6	21.9
	14	6	10.5	34.8
	15	12	2.6	10.4
Odense	26	22	1.0	1.8
	27	5	2.1	4.8
Mean values				
Sabro		58	8.3	33.3
Kratbjerg		60	5.1	16.2
Odense		27	1.2	2.3

By comparing table 3.1 and k_c in table 3.2 we find sufficient agreement between the two methods. Taking into account the differences in stress levels, the oedometer values seem to be a little too great. But we have also used the method described above in the new oedometer and here the drainage is not monoaxial. This simplification consequently gives errors of minor importance.

Axi-Symmetrical Consolidation

The variation of settlement with time can at present only be calculated on the basis of the theory of elasticity, because it gives a unique relation between stresses and strains in a semiinfinite solid caused by loaded areas at the surface. If we had a stress-strain relationship for soil describing all the wellknown phenomena, such as non-linearity between stresses and strains, differences between primary loading, unloading and reloading, creeping effects etc., we should of course use this relationship instead of the theory of elasticity. At present we have to solve the problems by assuming elasticity and afterwards discuss the differences between an elastic solid and a soil and how they influence the solution of the problem, e.g. the rate of consolidation.

The basic assumptions have already been pointed out in the previous chapter, because the determination of the coefficient of permeability by means of oedometer tests also implies the theory of elasticity. It has been shown that this theory leads to reasonable results.

The problem treated here deals with circular foundations (diameter D) on the soil surface, and loaded instantly, the load being constant in the consolidation period.

The solution of drainage problems is most appropriately represented by the so-called "equivalent drainage path" H_q, which, inserted in the normal drainage equation

$$t = \frac{\gamma_w H_q^2}{k \cdot K} T = \frac{H_q^2}{c_k} T$$

gives the correct value of t_c, if it is assumed that T is the usual function of the degree of saturation U. If we use a $\sqrt{t}$, log t scale we have

$$t_c = \frac{\pi}{4} \frac{H_q^2}{c_k}$$

The basic equation for consolidation in three dimensions is given by Biot (1941):

$$c_k \nabla^2 \varepsilon_v = \frac{\delta \varepsilon_v}{dt} \qquad (3.10)$$

where ε_v is the volume change. Since the total stresses do not change during consolidation, this can also be expressed as

$$c_k \nabla^2 h = \frac{\delta h}{\delta t} \qquad (3.11)$$

The problem is simplified here to the case of axial symmetry and the operator ∇^2 is then equal to

$$\nabla^2 = \frac{\delta^2}{\delta r^2} + \frac{1}{r} \frac{\delta}{\delta r} + \frac{\delta^2}{\delta z^2}$$

where r, z (and Θ) are polar coordinates.

The solution will be dimensionless when using the time factor $T = \frac{c_k \cdot t}{D^2}$, which is a pure number.

Boundary Conditions For Drainage

1. At the time $t = 0$ the excess pore water pressure can be calculated by means of Boussinesq's formulas.

2. At any time $t > 0$ the excess hydraulic pressure at the pervious part of the surface is zero, and at the impervious boundaries the gradient of excess hydraulic pressure normal to the boundary is zero.

3. After a very long time the hydraulic gradients have become zero.

The under-side of a concrete foundation consists of a rather thin layer of massed concrete with a large water-cement ratio. The permeability of the concrete is not known with any accuracy. For foundations on moraine clay we assume, however, that the base is impervious.

Boundary Conditions For Deformations

In the case of a semi-infinite elastic solid uniformly loaded over a circular area of the surface we get a problem without further conditions.

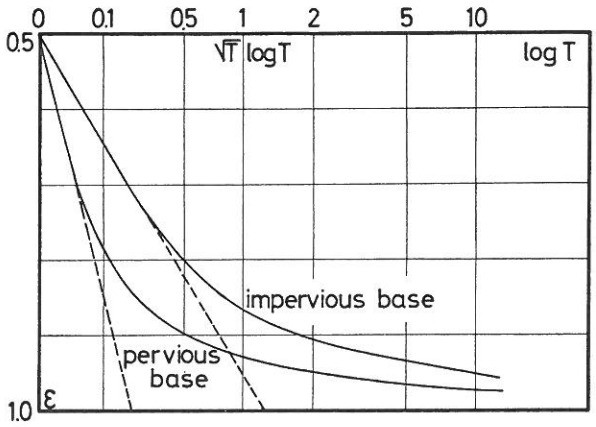

Fig. 3.13 Time curves for a uniformly loaded area on the surface of an elastic solid ($\mu = 0$) (de Josselin de Jong (1957)).

A solution is here given by de Josselin de Jong, and time curves can be seen on fig. 3.13. Part of the settlement appears immediately, due to shear deformations. When $\mu = 0$, $\varepsilon_i = 0.5\varepsilon_c$, increasing to $\varepsilon_i = \varepsilon_c$ when $\mu = 0.5$. The degree of consolidation U may here be defined as

$$U = \frac{\varepsilon - \varepsilon_i}{\varepsilon_c - \varepsilon_i}$$

De Josselin de Jong's solution can be expressed as follows for

impervious base $T = 1.2\ U^2$ for $U < 0.5$
or $H_q = 1.24\ D$

pervious base $T = 0.2\ U^2$ for $U < 0.4$
or $H_q = 0.50\ D$

It will be seen that the influence of the boundary conditions here gives a factor of 6.

In problems where more or less rigid elements are involved further boundary conditions are necessary. A typical problem of this kind is the case of a semi-infinite solid loaded by a rigid circular plate.

The additional boundary condition is:

4. The surface of the solid under the plate remains plane.

The stress distribution on the plate is not uniform but increases to infinity under the edge of the plate. The initial pore-water pressure under the edge is also infinite and near the edge much greater than in the centre line (fig. 3.18). Ignoring boundary condition no. 4 the pore water escapes first from the solid near the edge of the plate. The surface of the solid will then settle near the edge and the plate will stand on the top of the solid in the centre line (fig. 3.14). Condition no. 4 thus gives a variation in the stress distribution. In the first period the stresses at the middle of the plate will increase and later on the centre will again be somewhat unloaded.

Fig. 3.14 Without boundary condition for deformations the solution of the drainage for a rigid plate would lead to absurd results.

The deformations can be determined as follows:

in the drained state

$$\varepsilon_x = \frac{1}{E}(\bar{\sigma}_x - \mu(\bar{\sigma}_y + \bar{\sigma}_z))$$

and the analogous equations;

in the undrained state

$$\varepsilon_x = \frac{2(1+\mu)}{3E}(\bar{\sigma}_x - \frac{1}{2}(\bar{\sigma}_y + \bar{\sigma}_z))$$

$$= \frac{1}{E_u}(\sigma_x - \frac{1}{2}(\sigma_y + \sigma_z))$$

and the analogous equations.

The stress distribution under a rigid plate does not depend on E and μ, and the undrained state can be described by means of $E = E_u$ and $\mu = \frac{1}{2}$. This means that both in the undrained and drained state the stress distribution is the same and therefore the variation of the stresses during consolidation is reversible.

A similar problem is the case of a cylindrical elastic body with loading at the end surface with rigid plates and prevented lateral deformations, but the drainage may for instance take place through a part of the end-surfaces only. (The new oedometer des-

cribed in Paper no. 1). The boundary condition for deformations is that the end-surfaces remain plane. The solution will not be treated here.

Numerical Solution

A part of the semi-infinite solid can be represented by a rectangular network with the mesh widths Δr and Δz, and the excess pore water pressure is then represented by the hydraulic potential in the node points.

The hydraulic potential at the time t is given and we want to calculate it at the time $t + \Delta t$.

Formula 2.21 can be approximated by

$$h_{r,z}^{t+\Delta t} - h_{r,z}^{t} = \frac{\Delta t \cdot c_v}{m^2}(h_{r+1,z} + h_{r-1,z} + h_{r,z+1} + h_{r,z-1} - 4h_{r,z} + \frac{m}{2r}(h_{r+1,z} - h_{r-1,z})) \qquad (3.12)$$

where

$$\frac{c_v}{m^2} = \frac{c_{vr}}{\Delta r^2} = \frac{c_{vz}}{\Delta z^2}$$

i.e. in the isotropic case is assumed $\Delta r = \Delta z$.

If mh describes the factor in the bracket formula (3.12) can be written

$$\Delta h = \frac{\Delta t \cdot c_v}{m^2} \cdot mh$$

and it is noted that for $r = 0$, we have $mh = 4h_{r+1,z} + h_{r,z+1} + h_{r,z-1} - 6h_{r,z}$.

Since the values of h are known at the time t it seems to be most convenient to let the h values at the right side of the equation (3.12) correspond to the time t. $h_{r,z}^{t+\Delta t}$ can then be directly calculated in each node successively. This method is not stable for $\frac{\Delta t \cdot c_v}{m^2} > 1/8$.

Another method is to let the h values correspond to the time $t + \Delta t$, and we then get one equation per node with five unknown in each. This method is very time-consuming, but is always stable.

Both methods give one-sided deviations but on each side of the correct solution. A better one is to interpolate between these two methods by using $\frac{\Delta h}{\Delta t} = (1 - \varepsilon)\frac{\Delta h^t}{\Delta t} + \varepsilon \frac{\Delta h^{t+1}}{\Delta t}$. This is always stable for $\varepsilon \geq \frac{1}{2}$ and gives nearly correct results.

The interpolation method can be used in *EDP* calculations in a very practical way for a simple iteration routine. First we find Δh by the first method node for node by $\Delta h = \frac{t \cdot c_v}{m^2} \cdot mh_t$ and after that we repeat the same procedure on Δh instead of h. This process is called mh_t^2. mh_t^3, . . . mh_t^n can be described in the same way. The interpolation method can be described by

$$h_{t+1} = h_t + \frac{\Delta t \cdot c_v}{m^2} \cdot mh_t + 0.5\left(\frac{\Delta t \cdot c_v}{m^2}\right)^2 mh_t^2 + \ldots . \; 0.5^{n-1}\left(\frac{\Delta t \cdot c_v}{m^2}\right)^n mh_t^n$$

but is of course only a second order approximation with maximum accuracy for $n = 3$.

For $n = 1$ the one-sided deviation is 1 %, for $n = 3$ only 1 ‰.

This formula has been used in the calculations.

Rigid, Circular Plate

The circular plate is divided into concentric, circular rings, each of a width equal to the mesh width m of the network.

At the time $t = 0$ the volume changes are zero, $\bar{\sigma} = 0$ and the pore water pressure $u = \gamma_w \cdot h = \frac{1}{3}\Sigma\sigma$.

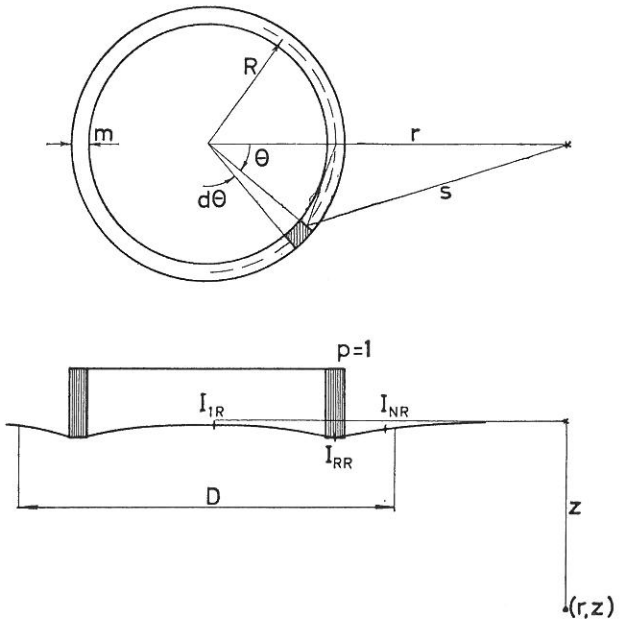

Fig. 3.15 A circular ring on the surface of an elastic solid.

For a small unit-loaded element of the ring we have (fig. 3.15)

$$du = \frac{z(1 + \mu)}{3\pi(s^2 + z^2)^{3/2}} m R \, d\Theta$$

and by integration

$$u_{r,z} = \frac{C \cdot A^{-3/2}}{1 - B/A} E\left(\sqrt{\frac{B}{A}}\right)$$

E is the complete elliptical integral of the second kind, $A = (r + R)^2 + z^2$, $B = 4rR$ and $C = \frac{4}{3\pi} \cdot z(1 + \mu) m R$.

If $z = 0$, $C = 0$ and $u_{r,o} = 0$. This is correct, except under the ring where $u = \frac{2}{3}(1 + \mu)$.

The vertical normal stress σ_z can be expressed in a similar way but cannot be simply reduced and is then calculated numerically.

For $z = 0$, $\sigma_z = 0$ except under the ring, where $\sigma_z = 1$.

The vertical undrained deformation ε_z of a little solid element is found by

$$\varepsilon_z = \frac{1+\mu}{E}(\sigma_z - u)$$

and the vertical deformations of the surface can now be calculated by integration along vertical lines.

The deformation condition that all the rings should have the same settlement gives, by means of influence numbers defined as the settlements I_{NR} shown in fig. 3.15, the stress distribution under the rings (fig. 3.17).

In *the drainage period* the total stresses are kept constant and we have

$$\frac{\delta \varepsilon_z}{\delta t} = -\gamma_w \frac{1-2\mu}{E} \frac{\delta h}{\delta t}$$

This means that the increment of the vertical deformation is proportional to the reduction of pore water pressure. After a time interval Δt we can calculate the reduction of the hydraulic potential by means of formula (3.12) and the changes in vertical deformation of the surface under the plate. The deformation condition gives now the undrained changes of the stress distribution and this again changes the hydraulic potentials somewhat.

Hereafter follows a new drainage calculation.

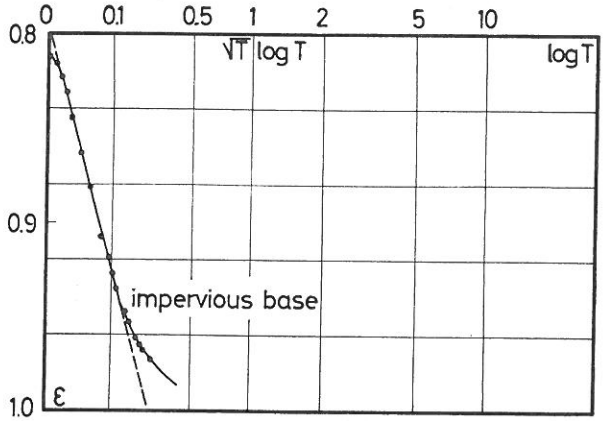

Fig. 3.16 Time curve for the settlement of a rigid plate loading the surface of an elastic solid ($\mu = 0.3$).

By the method described above we can calculate a time curve step by step as shown in fig. 3.16. The base of the plate is assumed impervious, corresponding to moraine clay. The solution can be expressed by

$$T = 0.25\, U^2 \text{ for } U < 0.75$$
$$\text{or } H_q = 0.56\, D$$

Part of the settlement appears immediately. When μ is zero, ε_i is nearly $\frac{2}{3}\,\varepsilon_c$, increasing to $\varepsilon_i = \varepsilon_c$ for $\mu = \frac{1}{2}$.

Fig. 3.17 shows the variation of the stresses under the plate during consolidation. Fig. 3.18 shows the excess pore pressure field at the time $t = 0$ and for three different degrees of consolidation. It will be seen that the maximum of excess pore pressure is situated at a nearly constant depth in a long period ($0 < U < 0.75$). This is caused by the changing of the stress distribution and makes the equivalent drainage path nearly constant and the law $T = 0.25\, U^2$ valid for $U < 0.75$.

It will be seen that the consolidation time is 5 times shorter for a rigid plate than for a uniformly loaded one.

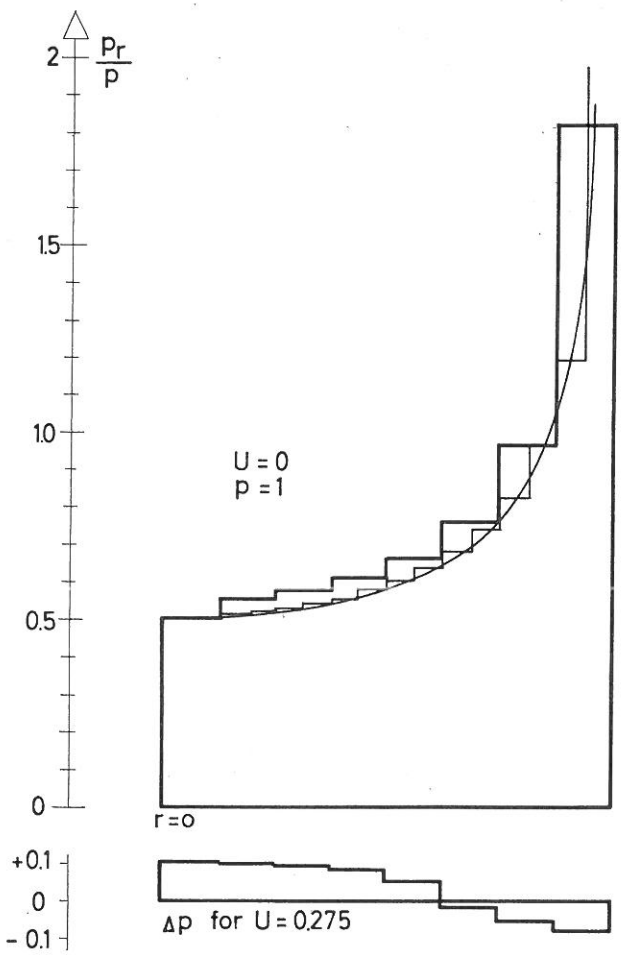

Fig. 3.17 Stress distribution under a plate with 8 rings or 16 rings compared with the theoretical distribution. The figure also shows the variation of stresses in the first period of consolidation ($U = 0$–0.275).

Deviations From Theory

We have shown how the theory of elasticity can be used to calculate the drainage of a rigid plate situated on the surface of an elastic solid.

However, the behaviour of a soil is not elastic and therefore we have to investigate the influence of the deviations from the theory. Here two very important factors should be pointed out.

Increasing Stiffness With Depth

Normally the soil grows firmer with increasing depth. For a preconsolidated soil the variation of the

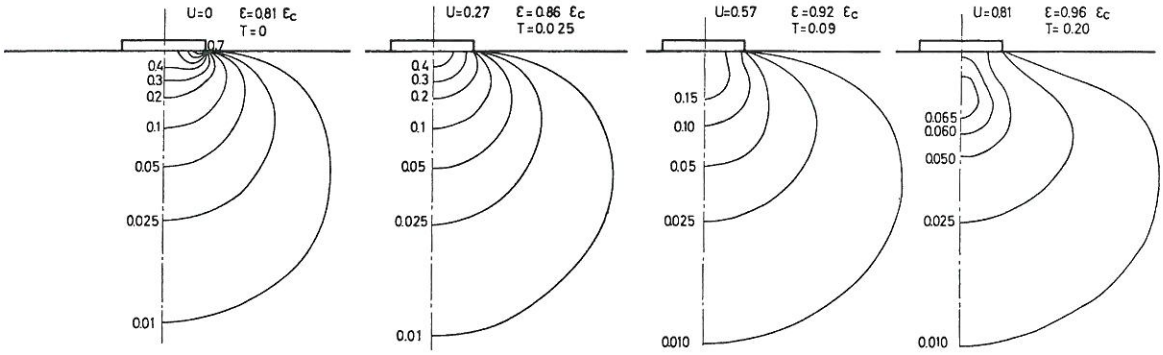

Fig. 3.18 Excess pore water pressure under a rigid plate on the surface of an elastic solid ($\mu = 0.3$) during consolidation. Mean load 1 t/m².

modulus of compression with the overburden pressure is nearly linear.

$$K = K_{fl}\,(1 + \alpha \cdot Z/D) \qquad (3.13)$$

where *fl* denotes foundation level.

It is assumed that Boussinesq's formulas for the stress distribution in an elastic solid caused by a point load on the surface are still valid. This is normally accepted for settlement calculations.

When calculating the deformations corresponding to the stresses we used formula (3.13), which gives a different stress distribution on a rigid plate and a different settlement of the plate. This is also accepted for settlement calculations, but sometimes formula (3.13) has a more complicated form.

The assumption (3.13) or a modified form leads to usable methods for settlements calculations and is therefore also used when determining consolidation times.

Numerical calculations similar to those mentioned in the previous chapter are carried out with $\alpha = 0.8$, 2.4 and 7.2. The results presented in fig. 3.19 show the variation of the equivalent drainage path with α. For the calculation of t_c, K_{fl}, H_q and $T = \pi/4$ should be used.

Since the permeability of the soil is relatively large, it is very difficult to observe time curves for normal buildings. But in one case we succeeded in doing so, and this is described in the next section.

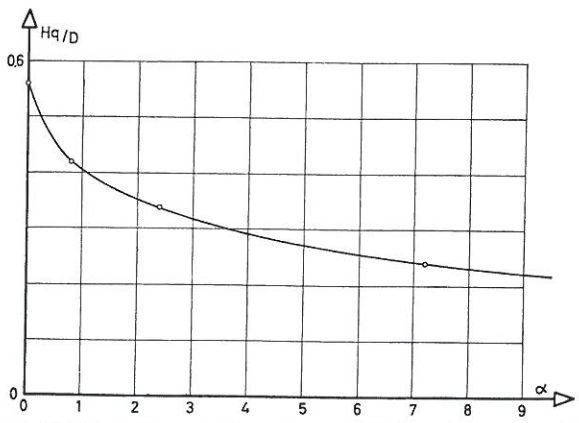

Fig. 3.19 When the modulus of consolidation increases with depth (formula 3.13) the equivalent drainage path decreases.

Observations

Settlements observations have been carried out on a spherical ammonia tank in Odense, Denmark. The diameter of the circular foundation was 12 m and it was founded directly on the surface of a moraine clay at level +1.8 m. The ground water level was usually about +1.2 m. The modulus of compression at level +1.8 m was $K_{fl} = 6100$ t/m² and increased very much with the depth. α is determined at 6 (formula (3.13)).

The measuring system for the settlements was arranged so that it was possible to determine the deformation of the upper 2.4 m and the upper 7.5 m of the soil by means of a dial gauges and the total settlements in a precision-levelling.

The settlements were observed from the very beginning. The weight of the construction was 1000 t, but the construction period was much longer than the drainage period (several months) and a time curve could not be observed. Before filling the tank with ammonia, it was filled with 5200 m³ water in less than two days (150 m³ ph). After emptying the tank it was refilled with ammonia and in one case the load was constant for 700 hours. The load increment of 1230 t was added in 18 hours, so this time curve corresponds as closely as possible to the theoretical assumptions.

The time curves are shown in fig. 3.20. The theoretical curves for the vertical deformations of the two layers and the total vertical deformation are also shown for an elastic solid. These curves show the variation of the consolidation time with the thickness of the considered upper layer of the soil. It will be seen that the variations observed are similar to the theoretical ones. The settlements measured by means of dial gauges are very accurate compared with the results of levellings. If the last result of a levelling is ignored we get the following consolidation times:

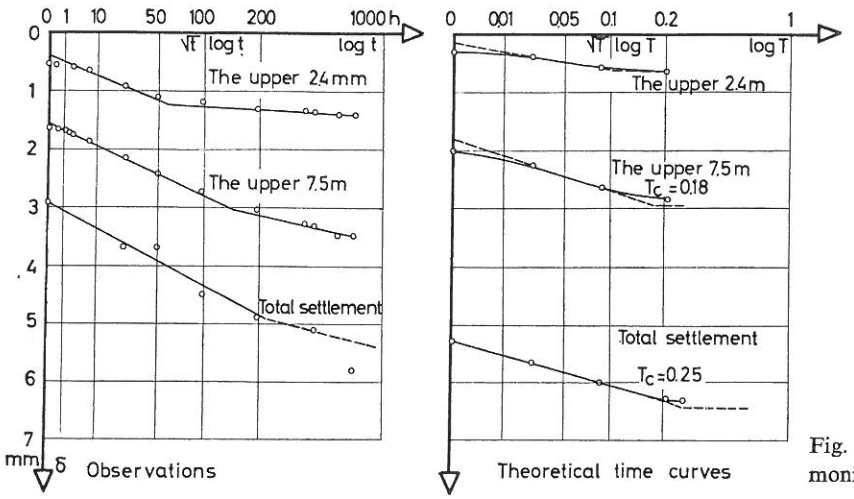

Fig. 3.20 Settlement observations of an ammonia tank.

for the upper 2.4 m: $t_c = 60\,h$
for the upper 7.5 m: $t_c = 130\,h$
for the foundation : $t_c = 220\,h$

The theoretical curves show that the consolidation time for the foundation should be 2.5 times longer than for the upper 2.4 m and 1.4 times longer than for the upper 7.5 m.

This gives three values of the consolidation time observed for the foundation: $t_c = 150$, 180 and 220 h.

The coefficient of permeability of the moraine clay is determined by means of oedometer tests at three different depths:

$$z/D = 0 \quad k_{10} = 6.5 \cdot 10^{-10} \text{ m/sec}$$
$$z/D = 0.5 \quad k_{10} = 11 \cdot 10^{-10} \text{ m/sec}$$
$$z/D = 1 \quad k_{10} = 9.5 \cdot 10^{-10} \text{ m/sec}$$

The permeability is not a constant as assumed, but here the mean value of $k_{10} = 9 \cdot 10^{-10}$ m/sec is used. Now the coefficient of consolidation c_k can be determined

$$c_{k,fl} = K_{fl} \cdot k/\gamma_w = 5.5 \cdot 10^{-6} \text{ m}^2/\text{sec}$$

and by means of fig. 3.19 we get $H_q = 0.26\,D = 3.1$ m.

The theoretical consolidation time is then

$$t_c = \frac{\pi}{4} \cdot \frac{3.1^2}{5.5} \cdot 10^6 \text{ sec} = 385\,h$$

or nearly two times the observed one.

This result agrees reasonably with the observations, but the calculated consolidation time is still too large.

The grain silo of "Muus" was filled with grain in three weeks and an undrained state occurred. Settlement observations show a consolidation time t_c of about 200 days, whereas calculations show $t_c = 80$ days, i.e., less than half the observed value in this case.

These two observations show that the approximations and assumptions made in this paper are reasonable.

Expansion before rupture

A preconsolidated soil expands under failure conditions. The expansions begin for shear stresses nearly half as great as the shear stresses at failure.

If the soil has been loaded with a certain shear stress before, it will probably not expand or only very little for shear stresses smaller than those in the preloading. In the observation mentioned below the preloading was 6200 t during the testing of the construction with water, and the actual load was 5000 t. In this case the expansion of the soil will be of minor importance.

But the plates in tests carried out on moraine clay had not been preloaded and here the influence of the expansion is very important.

Regarding the theoretical excess pore water pressure just after the application of the load, as shown in fig. 3.18, it will be seen that the greatest pore pressures occur under the edge of the plate, and here we also have the greatest shear stresses. This means that instead of pore pressure in these parts of the soil there is pore suction. The dimensions of the suction part of the soil depend of course on the loading of the plate. For smaller loads the suction part is only small and deviation from the theory is negligible. For increasing loads this part will expand and the drainage of the water is transformed into an internal process, where water to some extent flows from some parts of the soil to others.

It is not yet possible to give a calculation method in this case, but by means of plate tests one can investigate this effect.

It is usually not possible to determine the consolidation time for plate tests, because it is so small. Only a few plate tests should therefore be mentioned here.

The diameters of these plates are 0.5, 0.3 and 0.15 m and the tests were performed on Kratbjerg moraine clay with a coefficient of permeability of $20 \cdot 10^{-10}$ m/sec (Table 3.2). The consolidation time t_c is shown in fig. 3.21 as a function of p/p_f, where p is the mean load and the suffix f denotes failure. It will be seen that t_c decreases by a factor of 3–7.

The consolidation time for $p = 0$ should be calculated by means of the theory. α is very small for plate tests and here we use $\alpha = 0$. For small values of p/p_f the settlement of the plate is proportional to the applied mean load. Consequently the modulus K can be taken as a constant. We get:

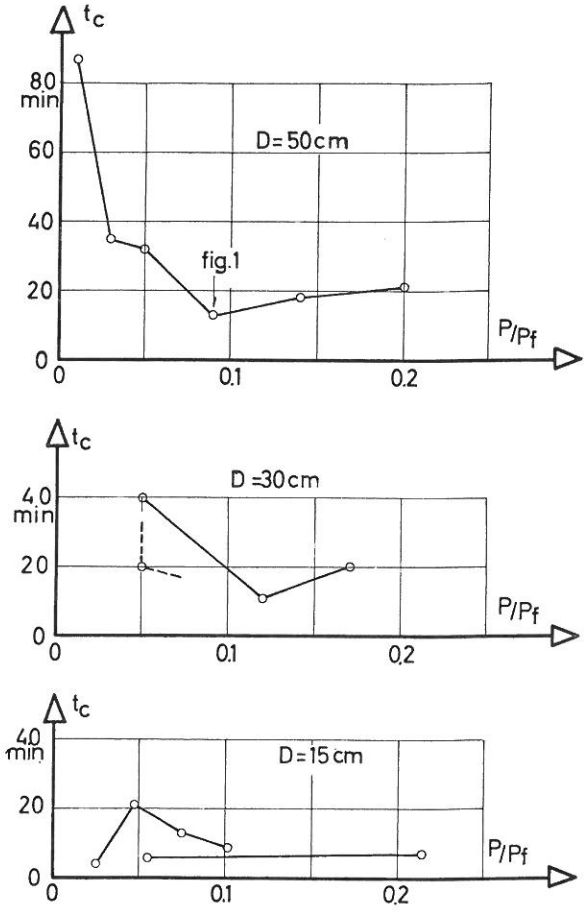

Fig. 3.21 Results of plate tests.

50 cm plate	$K = 15500$ t/m²	$t_c = 34$ min
30 cm plate	$K = 9800$ t/m²	$t_c = 19$ min
15 cm plate	$K = 8200$ t/m²	$t_c = 6$ min

For plate tests too we obtain close agreement between the theory and the tests for small loads (fig. 3.21).

Summary

This paper deals with the determination of the consolidation time t_c for circular footings on the surface of preconsolidated moraine clay.

The determination of the coefficient of permeability k in the laboratory involves some sources of error, which, when uncorrected, lead to too small values of k.

It is shown that, if the permeability is big enough, oedometers containing too small samples give too small values of k. An example shows that a factor of 6 is involved.

Darcy's law appears to be valid for moraine clay, but $c_v = k \cdot K/\gamma_w$ varies somewhat. Comparison of k measured in permeability tests and determined on the basis of oedometer tests performed with the same sample shows that oedometer tests nevertheless give reasonable results (fig. 3.7).

If the sample in the oedometer is not fully saturated, the pore liquid is compressible and the classical theory gives too small values of k. A method taking this into account is described and verified by means of special permeability tests (table 3.1 and 3.2). The factor of error is for moraine clay 2 to 4 depending on the degree of saturation. A normal fat clay is usually fully saturated.

A similar effect of the saturation degree is observed in permeability tests, in which air bubbles prevent the water from flowing (fig. 3.9).

The coefficient of permeability determined in oedometer tests corresponds to very small amounts of water flow. Under foundation, however, some parts of the soil will be flowed through by larger amounts of water. But permeability tests on moraine clay show that the measured k is independent of the amount of pore water flow.

Calculation on the basis of the theory of elasticity can be carried out if the boundary conditions are known. De Josselin de Jong (1957) has shown that the difference between pervious and impervious base gives a factor of 6 for a uniformly loaded, circular area. It is therefore very important to take this boundary condition into account.

For rigid circular plates numerical calculations have been made for impervious base. The boundary condition for deformations causes a change of the stress distribution on the plate and thus accelerates the drainage nearly 5 times.

Two important differences between the theory of elasticity and the behaviour of a soil are pointed out.

1. The coefficient of elasticity increases with depth. The stresses according to Boussinesq's formuals are used, but the strains are calculated by means of the soil properties. Numerical calculations show the variation of the equivalent drainage path H_q (fig. 3.19) to be used with the modulus of compressibility K at foundation level. When a mean value of K, defined by $K_m = \frac{\pi}{4} \cdot p_m \cdot \frac{D}{\delta}$, and H_q corresponding to constant K are inserted, nearly the same result is obtain-

ed. The difference between these two methods is only 5–10 %.

2. Preconsolidated clays expand under great shear stresses. Consequently pore water suction exists in that part of the soil which according to the theory should have maximum excess pore water pressure. Plate tests show a nearly constant modulus of settlement for $p/p_f < 0.25$ but nevertheless a decreasing consolidation time, owing to the creation of areas of pore water suction and the increasing influence of internal drainage. The observations show that this effect gives a factor of 2–3 (fig. 3.21).

By taking all the above-mentioned factors into account we obtain for the consolidation time good agreement between theory and observations, as demonstrated by settlement observations and plate tests.

References

Barden, L. and McDermott, R. J. W. (1965): Use of free ends in triaxial testing of clays. Proc. ASCE Vol. 91 SM6.

Biot, M. A. (1941): General theory of three-dimensional consolidation. J. App. Phys., 12, 155.

Bishop, A. W. and Henkel, D. J. (1957): The measurement of soil properties in the triaxial test. Arnold, London 1957.

Bishop, A. W. and Gibson, R. E. (1963): The influence of the provisions for boundary drainage on strength and consolidation characteristics of soil measured on the triaxial apparatus. Spec. Tech. Publ. No. 361 ASTM 1963.

Bishop, A. W. and Blight, G. E. (1963): Some aspects of effective stress in saturated and partly saturated soils. Géotechnique, Sept. 1963 p. 177.

Bishop, A. W. and Green, G. E. (1965): The influence of end restraint on the compression strength of a cohesionsless soil. Géotechnique Vol. XV, 2 p. 243.

Boussinesq, J. (1885): Application des potentiels a l'étude de l'équilibre et du mouvement des solides élastiques. Paris 1885.

Brooker, E. W. (1965): Earth pressures at rest related to stress history. Can. Geotech. J. Vol. III no. 1.

Burmister, D. M. (1945): General theory of stresses and displacements in layered systems. J. Appl. Phys., 16, 5.

Carillo, N. (1942): Simple two and three dimensional cases in the theory of consolidation of soils. Cambr. Mass.

Dansk Ingeniørforening (1966): Code of Practice for Foundation Engineering. Danish Geot. Inst. Bull. 22.

Fröhlich, O. K. (1934): Druckverteilung im Baugrunde. Springer, Wien.

Gibson, R. E. and McNamee, J. (1957): The consolidation settlement of a load uniformly distributed over a rectangular area. Proc. 4th Int. Conf. Soil. Mech. Vol. 1 p. 297, London.

Hansbo, S. (1960): Consolidation of clay with special reference to influence of vertical sand drains. Proc. Swedish Geot. Inst. no. 18.

Hansen, J. Brinch og Lundgren, H. (1958): Geoteknik. Teknisk Forlag, Copenhagen.

Hansen, J. Brinch (1961): A general formula for bearing capacity. DGI-bull. 11.

Hansen, J. Brinch (1961): A model law for simultaneous primary and secondary consolidation. DGI-bull. 13.

Henkel, D. J. and Gilbert, G. D. (1952): The effect of the rubber membrane on the measured triaxial compression strength of clay samples. Géotechnique Vol. III p. 20.

Henkel, D. J. (1956): The effect of overconsolidation on the behaviour of clays during shear. Géotechnique Vol. VI p. 139.

Hvorslev, M. J. (1937): Über die Festigkeitseigenschaften gestörter bindiger Böden. Ing. vid. Skrift. A45, Kbh.

Jacobsen, M. (1967): The undrained shear strength of preconsolidated boulder clay. Proc. Eur. Congr. Soil Mech. Vol. I p. 119, Oslo.

Josselin de Jong, G. de (1957): Application of stress functions to consolidation problems. Proc. 4th. Int. Conf. Soil Mech. Vol. I p. 320, London.

Kezdi, A. (1958): Beiträge zur Berechnung der Spannungsverteilung im Boden. Der Bauingenieur 33, 1958 p. 54.

Mandel, J. (1953): Consolidation des sols. Géotechnique Vol. III p. 287.

Meyerhof, G. G. (1950): The bearing capacity of sand. Ph. D. thesis. Univ. of London.

Roscoe, K. H. et al. (1958): On the yielding of soils. Géotechnique Vol. VIII p. 22.

Roscoe, K. H. and Schofield, A. N. (1963): Mechanical behaviour of an idealized »wet-clay«. Proc. Eur. Congr. Soil Mech. Found. Eng., Wiesbaden.

Rowe, P. W. and Barden, L. (1964): Importance of free ends in triaxial testing. Proc. ASCE Vol. 90, SM1 p. 1.

Skempton, A. W. (1948): The effective stresses in saturated clays strained at constant volume. Proc. 7th Int. Congr. App. Mech., Vol. 1 p. 378.

Skempton, A. W. (1954): The pore-pressure coefficients A and B. Géotechnique Vol. IV p. 143.

Skempton, A. W. and Bjerrum, L. (1957): A contribution to the settlement analysis of foundations on clay. Géotechnique, Dec. 1957, Vol. VII p. 168.

Taylor, D. W. (1942): Research on consolidation of clays. MIT 1942.

Timoshenko, S. and Goodier, J. N. (1951): Theory of elasticity. Mc Graw-Hill. New York.